# Experimental Evaluation of Mechanical Properties of 3d Carbon Fiber/Sic Composites Prepared By LSI

**Dr. S. Khadar Vali[1*] Dr. P. Ravinder Reddy[2] Dr. P. Ram Reddy[3]**

1. Professor and Head, MED, M. J. College of Engineering and Technology, Banjara Hills, Hyderabad, India.
2. Professor and Head, MED, Chaitanya Bharati Institute of Technology, Hyderabad, India.
3. Former Registrar, JNTU Hyderabad, Presently Director, Malla Reddy Institute of Engg. & Technology, Hyderabad, India

**Abstract**

The structural engineer needs to be familiar with the property of the composite material structures. The behavior of ceramic composite material under impact load plays a pivotal role in designing such structures. An impact test is a test for determining the energy absorbed in fracturing a test piece at high velocity. The impact resistance of a part is, in many applications, a critical measure of service life. In the current work, an attempt is made to present the dynamic behavior of the advanced ceramic composite material, i.e., 3 Dimensional Carbon-Silicon Carbide (3D C-SiC) under the impact, tensile and flexure loads and the mechanical properties, viz., Impact Strength, Tensile Strength and Flexural Strength are determined. 3D C-SiC composite specimens with a fiber volume fraction of 40% are prepared by Liquid Silicon Infiltration (LSI) process to conduct the required experiments for evaluating the mechanical properties. The experimental results of impact, tensile, flexure and shear strengths recorded during the tests are 26.82 kJ/m$^2$, 70.2 MPa, 230.3 MPa and 30.5 MPa respectively.

**Keywords:** Carbon Silicon Carbide (C-SiC), Impact strength, Liquid Silicon Infiltration (LSI)

## 1. Introduction

The minimum knowledge required about a material to characterize fracture properties comes from a force-time (or force-displacement) diagram. When performing a test with an instrumented falling weight, it is possible to record the force acting on the specimen throughout the impact. Silicon carbide matrix based composites exhibit promising mechanical properties at high temperatures and offer very good oxidation and thermal shock resistance. They are finding increasing applications in aerospace, defense and industries. Carbon fiber-reinforced SiC matrix composites are preferred to C-C composites for oxidizing and highly erosive environment. C-SiC composites are used up to 1500$^0$ C for long durations and up to 2000$^0$C for short durations. The mechanical properties of the fiber-reinforced composites can be tailored by adjusting fiber volume fraction and fiber orientation to meet the needs of the application. C-SiC composites retain mechanical strength up to 1700$^0$C. There are several methods to fabricate C-SiC composites, such as chemical vapor infiltration (CVI), slurry infiltration combined with hot pressing, polymer-infiltration-pyrolysis (PIP), etc. Among these methods, Liquid Silicon Infiltration (LSI) process offers many potential advantages such as single step process, low processing temperature, and near-net-shape processing. Continuous fiber reinforced ceramic matrix composites (CFCCs) are very interesting structural materials because of their higher performance and higher fracture toughness. For this reason, CFCCs are considered as the most potential to be used in advanced aero engines. Among the CFCCs, carbon fiber reinforced silicon carbide matrix composites (C-SiC) are most promising and have been receiving considerable interest. Many investigations have been conducted on two dimensional woven C-SiC composite materials. Recently, attention has been focused on three dimensional woven or braided ceramic matrix composite materials in order to meet mechanical property requirements along the thickness of the composites.

## 2. The LSI Process

The LSI (Liquid Silicon Infiltration) process consists of 3 stages. Beginning with a carbon fiber reinforced ceramic (CFRC) made of a coal tar pitch with high carbon content, a green-body preform is manufactured. This preform is then pyrolised under inert atmosphere at temperatures greater than 900$^0$C, converting the CFRC into a higher porous carbon-carbon (C-C) composite. In a final step, the porous material is infiltrated with liquid silicon under vacuum to manufacture the final C-SiC ceramic. The quality of the C-SiC materials is influenced by each individual processing stage.

## 3. Experimental Investigations

3D stitched preform is the simplest case of the 3D composites development; several layers of 8 H satin carbon fabric layers are stitched together with 6000 Carbon fibers to impart third direction reinforcement (Fig.1). The fiber volume fraction is worked out, taking into consideration the infiltration abilities of molten silicon vis-à-vis the thermo mechanical properties.

Fig. 1 The fixture of carbon fiber perform

## 4. Specimen Preparation And Test Methods

The instrument used to perform impact test is quite similar to drop weight machines. It is usually equipped with a piezoelectric or strain gauge load cell. The standard specimens are prepared with composition shown in Table 1.

Table 1 Composition of Carbon Silicon Carbide (C-SiC)

After preparing the C-SiC

| S. No. | Constituents | Percentage (% Vol.) |
|---|---|---|
| 1. | Carbon (Fibre) | 40% |
| 2 | SiC | 45% |
| 3 | Si | 10% |
| 4 | C | 5% |

specimens as per the required composition, they are cut into required sizes according to ASTM D256 standards (Fig. 2). The Izod impact tests are conducted using Fractovis drop weight instrumented impact tester acquired with a DAS 8000 WIN data acquisition system as shown in Fig. 3.

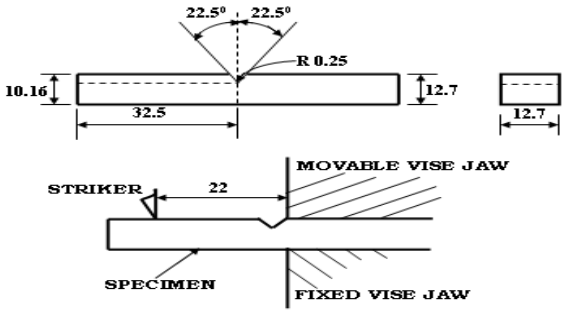


Fig. 2 Izod Test specimen geometry according to ASTM D 256 standards

(a) (b)

Fig. 3 Two Views of the Fractovis Instrumented Impact Tester

### 5.1 Measurement of Mechanical Properties- Impact Test

Mechanical properties of the C-SiC composite materials are characterized under impact loading to get the reliable design properties at room temperature. Instrumented impact tests on notched Izod samples are conducted as per ASTM D 256 standards to determine the energy absorbing capability and dynamic fracture behavior of the composite materials. The sample sizes are 10.16 x 12.7 x 32.5 mm and the impact velocity of 3 m/s is chosen. The dynamic fracture toughness ($\alpha_k$) is calculated using equation:

$$\alpha_k = \Delta W / bh$$

where $\Delta W$ is the absorbing energy of materials during impact processing, b and h are thickness and width of specimen respectively.

**5.2 Flexural Test**

This test method covers the determination of flexural properties of continuous fiber reinforced ceramic composites in the form of rectangular bars formed directly or cut from sheets, plates or molded shapes. According to ASTM C1341 standards, a three point loading system utilizing centre loading on a simply supported beam is chosen. The specimen geometry is shown in Fig. 4. The siliconised 3D C-SiC composite specimens shown in Fig. 5 are cut into sizes 6mm x15mm x100mm with support span length of 100mm along principal material direction and tested for three point bend test at room temperature to get flexural strengths.

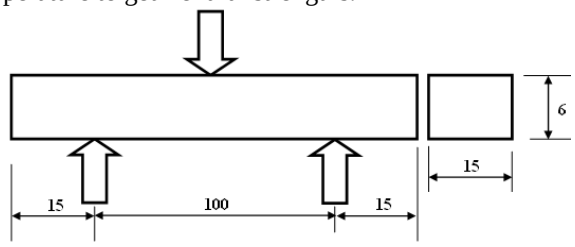


Fig.4 Specimen geometry for flexural test as per ASTM C1341 standards

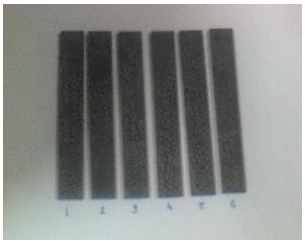

Fig.5 Specimens for Flexural and Shear tests

This test method applies primarily to all advanced ceramic matrix composites with continuous fiber reinforcement: one dimensional (1D), two dimensional (2D), and three dimensional (3D) continuous fiber architectures. In addition, this test method may also be used with glass matrix composites with continuous fiber reinforcement. However, flexural strength can not be determined for those materials that do not break or fail by tension or compression in the outer fibers. Test can be performed at ambient temperatures or at elevated temperatures. At elevated temperatures, a suitable furnace is necessary for heating and holding the specimens at the desired testing temperatures. In this test method, the flexural stress is computed from elastic beam theory with the simplifying assumptions that the material is homogenous and linearly elastic. This is valid for composites where the principal fiber direction is coincident or transverse with the axis of the beam. These assumptions are necessary to calculate a flexural strength value, but limit the application to comparative type testing such as used for material development, quality control and flexure specifications. Such comparative testing requires consistent and standardized test conditions, i.e., specimen geometry (thickness), strain rates, atmospheric test conditions. Flexure tests provide information on the strength and deformation of materials under complex flexural stress conditions. The geometry of the specimen must be chosen so that shear stresses are kept low relative to tension and compression stresses. This is done by maintaining a high ratio between the support span (L) and the thickness or depth (d) of the specimen. This L/d ratio is generally kept at the values of grater than or equal to 16 for 3- point flexure testing following the ASTM C1341 standards. If the span to depth ratio is too low, the specimen may fail in shear. The flexural specimens are tested in a properly calibrated universal testing machine (UTM) shown in Fig. 6 that can be operated at the constant rates of cross head motion over the range required. The system is equipped with a means for retaining the readout of the maximum load as well as the record of load verses deformation.

Fig. 6 Universal Testing Machine (UTM) to conduct Tensile, Flexure and Shear tests

The outer loading span and the desired test geometry determine the dimensions and geometry of the loading fixture. The fixture geometry, i.e., 3- point is selected. The thickness of the specimen to be tested determines the critical out span dimension of the loading fixture. The over all dimension of the specimen and required loading span are selected based on the specimen thickness, the desired test geometry, and the required span to depth ratio following ASTM C1341 standards. An autographic record of the applied load and the centre point deflection is obtained for the specified cross head rate. Either analog chart recorders or digital data acquisition systems may be used for this purpose, although a digital record is recommended for ease of subsequent data analysis. Ideally an analog chart recorder or plotter should be used in conjunction with digital data acquisition system to provide an immediate record of the test as a supplement to the digital record. Specimen width shall not exceed ¼*th* of the support span for specimens greater than 3mm in depth. The specimen shall be long enough to allow for overhang passed the outer supports of at least 5% of the support span, but in no case, less then 5mm on each end. Overhang shall be sufficient to minimize shear failures in the specimen ends and to prevent the specimen from the slipping through the supports at large centre point deflections. The test temperature is determined and recorded. The data acquisition is initiated and the load application is started. The test is continued until

the specimen breaks into two pieces. The maximum load is recorded. After completing the test, the action of the test machine and the data acquisition system is disabled. In addition to the location, carefully the mode of the fracture initiation and crack extension is noted. Fracture may initiate on the tensile (lower) face, on the compression (upper) face of the bar or by shear failure. The bar may fail by a sequential combination of modes. The tensile fracture crack may extend towards the neutral axis directly or may be deflected along low strength planes such as inter laminar regions.

***Flexural Stress (σ):***

When tested in flexure, a simple beam experiences maximum tensile stresses in the outer fibers and maximum compressive stresses in the inner fibers. The location of the maximum stress along the length of the beam is at the centre point for 3- point testing. Equation for calculating the flexural stress for the 3-point test is give as: Flexure Stress, $\sigma = 3PL/2bd^2$

Where, P = Load at given point in the test (N)
L = Support span (mm)
b = Specimen width (mm)
d = Specimen depth or thickness (mm)

***Flexural Strength ($\sigma_f$):***

The flexural strength is equal to the maximum stress in the outer fibers at the point of maximum load. It is calculated using the equation:

Flexural Strength, $\sigma_f = 3P_UL/ 2bd^2$

Where, $P_U$ = Maximum load in flexural test (N)
L = Support span (mm)
b = Specimen width (mm)
d = Specimen depth or thickness (mm)

**5. 3 SHEAR TEST**

Shear strength of 3D C-SiC composites is measured by conducting a three point bend test in the same UTM. The shear strength is calculated by the following equation.

$\square = 3P/4bh$

Where P is the fracture load (N), b and h are width and thickness of the specimen respectively.

**5. 4 TENSILE TEST**

The test specimens cut into sizes 3mm x 6mm x 100mm length according to ASTM C 1275 standards (Fig. 7) are shown in Fig. 8. They are fixed in the universal testing machine (UTM) to conduct tensile test by choosing the tensile fixture and properly adjusting the movable jaw so as to keep the gauge length of 25mm. The tensile load (P) is gradually applied along principal material direction. When the applied load reaches ultimate value, the specimen breaks catastrophically and the load falls to zero.

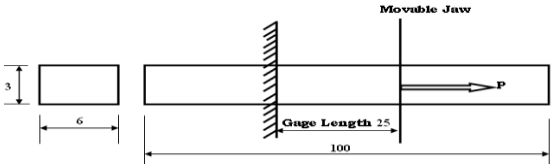


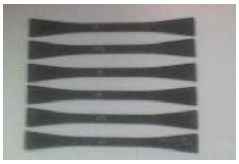

Fig. 7 Tensile test specimen geometry as per ASTM C1275 standards Fig.8 Tensile test specimens

The equation for calculating longitudinal strength in tension is expressed as:

$\sigma_t = P_U/A$

where $P_U$ = Ultimate load (kN)

A = Area of cross-section perpendicular to the direction of applied load

## 6. Results And Discussions

A typical Force-deformation curve recorded in the impact test is shown in Fig. 9. The test data for 7 sample specimens out of total 31 specimens tested is also shown in Table 2. First of all, when the striker touches the specimen the impact point is immediately accelerated from zero velocity to the initial velocity of the striker. This instantaneous acceleration, for the Newton's second law, causes a first peak of force named inertial peak (because of the inertial nature of this phenomenon). After this, strong oscillation force increases linearly. At low displacements, in fact any material can be considered elastic so that force is proportional to displacement (and therefore to time, if impact energy is high). When the specimen is affected by a great deflection, however, plastic deformation occurs: the load deformation curve deviates from linearity showing the characteristic yield region. Since the materiel chosen for test is C-SiC which is very hard and brittle, there is no noticeable yield region. When the material approaches its maximum deflection, fracture occurs and the measured force falls to zero. From the load displacement curve the evaluation is made on fracture toughness, i.e., the energy absorbed by the specimen during the fracture. The absorbed energy is a measure of material strength and the

ductility can be graphically represented as the area beneath the load-displacement curve. Further the impact strength is obtained by calculating the energy absorbed during fracture per unit cross sectional area of the specimen. The experimental values of fracture toughness and impact strength obtained during impact testing of the specimens with corresponding measured fiber volume fractions is given in Table 3. Fig. 10 and Fig. 11 clearly indicate the increase in fracture toughness and impact strength with the increase of fiber volume fraction in 3D C-SiC specimens. In the specimens tested, a considerable fiber pullout is observed (Fig. 12) indicating the increase of fracture toughness. It is obvious that 3D C-SiC composite materials exhibit an excellent impact damage tolerance because of Z-direction fibers. The measured properties of 3D C – SiC composites are compared with the properties of 2D C-SiC (available from literature) fabricated by different routes as shown in Table 4. The experimental results of impact strength of various specimens with 40 % fiber volume fraction are shown in Table 5. The flexural strengths calculated and maximum load recorded in the test for various specimens having fiber volume fractions 40 % is given in the Table 6. The broken specimen after conducting flexural test (Fig.13) shows lot of fibers being pulled out. This may be the reason for increase in flexural strength. The tensile strengths calculated for the ultimate loads recorded in the test for various specimens having fiber volume fraction of 40 % is shown in Table 7. Fig.14 shows the broken specimen after conducting tensile test. More or less a brittle failure can be observed from this figure which may be attributed to the fact of less tensile strength. The load deflection curves obtained in 3- point bend test for the specimens is shown in Fig.15. The load deformation curves obtained in the tensile test for the specimens are shown in Fig.16.The experimental results of shear strength is shown in Table 8.

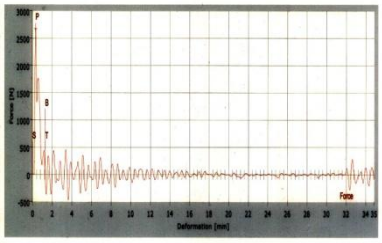

Fig. 9 Force-Deformation curves obtained in impact test up to failure

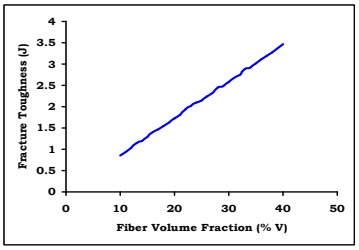


Fig.10 Fracture Toughness Vs Fiber VolumeFraction

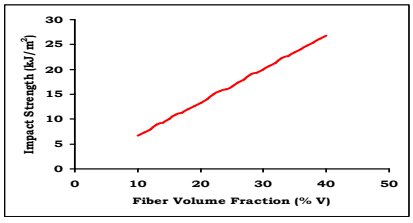


Fig. 11 Variation of Impact strength with fiber volume fraction

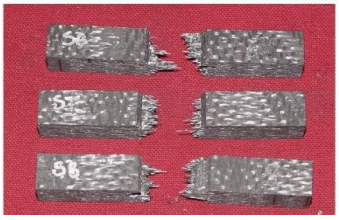

Fig.12 Fiber pull out in impact test

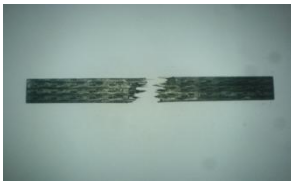

Fig. 13 Broken specimens in Flexural Test

Fig. 14 Broken specimen in Tensile Test

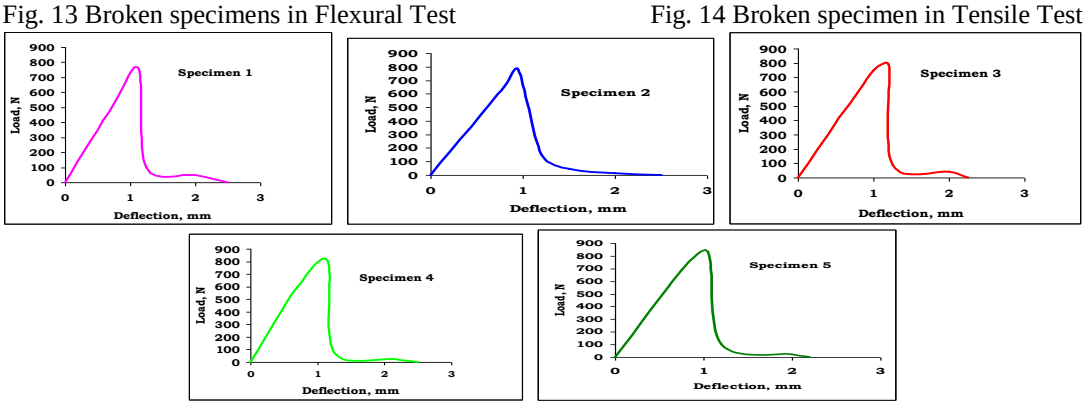


Fig.15 Load-Deflection curves of specimens obtained in Flexural Test

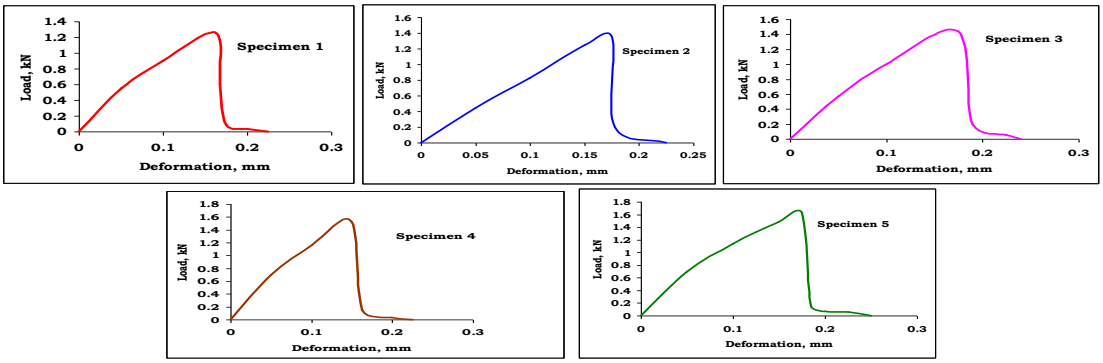


Fig. 16 Load-Deformation curves of specimens obtained in Tensile Test

Table 2 Impact Test Data of 3D C – SiC specimens

| | Sample data for Specimen No. 4 | | | Sample data for Specimen No.7 | | | Sample data for Specimen No.13 | | | Sample data for Specimen No.14 | | | Sample data for Specimen No.19 | | | Sample data for Specimen No.24 | | | Sample data for Specimen No.31 | | |
|---|---|---|---|---|---|---|---|---|---|---|---|---|---|---|---|---|---|---|---|---|---|
| | Start | Peak | Total | Start | Peak | Total | Start | Peak | Total | Start | Peak | Total | Start | Peak | Total | Start | Peak | Total | Start | Peak | Total |
| Deformation, d (mm) | 0.00 | 0.31 | 1.27 | 0.00 | 0.38 | 1.53 | 0.00 | 0.59 | 2.19 | 0.00 | 0.64 | 2.24 | 0.00 | 0.76 | 2.78 | 0.00 | 0.88 | 3.27 | 0.00 | 1.09 | 3.95 |
| Velocity, v (m/s) | 3.49 | 3.48 | 3.44 | 3.49 | 3.47 | 3.43 | 3.46 | 3.43 | 3.37 | 3.42 | 3.39 | 3.33 | 3.43 | 3.37 | 3.31 | 3.42 | 3.39 | 3.26 | 3.42 | 3.27 | 3.16 |
| Fracture Toughness (J) | 0.00 | 0.22 | 1.15 | 0.00 | 0.27 | 1.41 | 0.00 | 0.37 | 1.93 | 0.00 | 0.38 | 2.02 | 0.00 | 0.47 | 2.45 | 0.00 | 0.56 | 2.88 | 0.00 | 0.67 | 3.46 |
| Force (N) | 0.00 | 2683.51 | 0.00 | 0.00 | 2541.93 | 0.81 | 0.00 | 2370.06 | 0.00 | 0.00 | 2352.44 | 0.00 | 0.00 | 2224.96 | 0.55 | 0.00 | 2134.83 | 0.68 | 0.00 | 1832.25 | 0.55 |

Table 3 Variation of Fracture Toughness and Impact Strength with Fiber Volume Fraction of 3D C-SiC specimens

| | | | | | | | | | | | | | | | | | | | | | | | | | | | | | |
|---|---|---|---|---|---|---|---|---|---|---|---|---|---|---|---|---|---|---|---|---|---|---|---|---|---|---|---|---|---|
| Impact Strength (kJ/m²) | 6 65 | 7 31 | 7 97 | 8 91 | 9 30 | 9 99 | 10 93 | 11 31 | 11 99 | 12 65 | 13 29 | 13 96 | 14 96 | 15 65 | 15 95 | 16 65 | 17 32 | 17 98 | 18 99 | 19 32 | 19 98 | 20 65 | 21 31 | 22 32 | 22 64 | 23 40 | 24 10 | 24 80 | 25 42 | 26 11 | 26 82 |
| Specimen No. | 1 | 2 | 3 | 4 | 5 | 6 | 7 | 8 | 9 | 10 | 11 | 12 | 13 | 14 | 15 | 16 | 17 | 18 | 19 | 20 | 21 | 22 | 23 | 24 | 25 | 26 | 27 | 28 | 29 | 30 | 31 |
| Fiber Volume Fraction (% V) | 10 | 11 | 12 | 13 | 14 | 15 | 16 | 17 | 18 | 19 | 20 | 21 | 22 | 23 | 24 | 25 | 26 | 27 | 28 | 29 | 30 | 31 | 32 | 33 | 34 | 35 | 36 | 37 | 38 | 39 | 40 |
| Fracture Toughness (J) | 0 86 | 0 94 | 1 03 | 1 15 | 1 20 | 1 29 | 1 41 | 1 46 | 1 55 | 1 63 | 1 72 | 1 80 | 1 93 | 2 02 | 2 10 | 2 15 | 2 24 | 2 32 | 2 45 | 2 49 | 2 58 | 2 67 | 2 75 | 2 88 | 2 92 | 3 02 | 3 11 | 3 20 | 3 28 | 3 37 | 3 46 |

Table 4 Comparison of mechanical properties of 2D C–SiC composites (from literature) with experimental results of 3D C-SiC specimens

| Properties | Literature Values | | Experimental results of present work |
|---|---|---|---|
| | Unit | 2D C – SiC (LSI) | 3D C – SiC (LSI) |
| Fiber Volume | Vol. % | 40 –42 | 40 |
| Density | g/cc | 2.4 | 2.2 – 2.4 |
| Flexural Strength | MPa | 180 – 200 | 210 – 230 |
| Tensile Strength | MPa | 80 – 90 | 70 – 90 |
| Young's Modulus | GPa | 25 – 30 | 32 – 35 |

| | | | |
|---|---|---|---|
| Strain to failure | % | 0.25 – 0.35 | 0.20 – 0.28 |
| Impact strength | kJ / $m^2$ | 20 – 21 | 26 – 27 |

Table 5 Experimental results of impact strength of specimens with 40 % Fiber Volume Fraction

| Specimen No. | Fracture toughness (J) | Impact strength ($kJ/m^2$) From Experiment |
|---|---|---|
| 1 | 3.39 | 26.27 |
| 2 | 3.40 | 26.35 |
| 3 | 3.42 | 26.50 |
| 4 | 3.46 | 26.82 |
| 5 | 3.48 | 26.98 |

Table 6 Experimental results of flexural strengths of 3D C-SiC specimens

| Specimen No. | Max. load ($P_U$) recorded during flexural test (N) | Flexural strength, $\sigma_f$ (MPa) From Experiment |
|---|---|---|
| 1 | 757 | 210.2 |
| 2 | 780 | 216.6 |
| 3 | 789 | 219.2 |
| 4 | 805 | 223.6 |
| 5 | 829 | 230.3 |

Table 7 Experimental results of tensile strengths of 3D C-SiC specimens

| Specimen No. | Max. load ($P_U$) during tensile test (kN) | Tensile strength, $\sigma_t$ (MPa) From Experiment |
|---|---|---|
| 1 | 1.264 | 70.2 |
| 2 | 1.346 | 74.8 |
| 3 | 1.437 | 79.8 |
| 4 | 1.525 | 84.7 |
| 5 | 1.619 | 89.9 |

Table 8 Experimental results of Shear Strengths of 3D C-SiC specimens

| Specimen No. | Fracture load (P) in shear test (kN) | Shear strength, $\tau$ (MPa) |
|---|---|---|
| 1 | 3.38 | 28.16 |
| 2 | 3.64 | 30.33 |
| 3 | 3.55 | 29.58 |
| 4 | 3.66 | 30.50 |
| 5 | 3.52 | 29.33 |

The stress transfer capability of the interface between the fiber and matrix governs the mechanical properties of fiber reinforced composite materials. The interfacial compatibility is related to the interfacial shear stress, which characterizes the combination of stress necessary to de-bond the interface and the frictional forces developed at the interface. The 3D carbon preform is infiltrated by liquid silicon and the density obtained is 2.2–2.4 g $cm^{-3}$. The non-linear failure behavior is observed in the present composite material and it could also be observed that the failure of three dimensional C-SiC composite material occurred in a controlled manner. The average result of flexural strength is observed to be 220 MPa. The variation of failure behavior of composites is caused by alteration of the interfacial bonding between fiber and matrix. The tensile stress within the interfacial phase along the fiber radial direction is generated after the composite material is cooled down from the infiltration temperature to room temperature. It is easy for the carbon fiber to debond and be pulled out from the silicon carbide matrix. Above infiltration temperatures, the stresses at the interface become compressive which may lead to strong bond in between the constituents of the composite. Moreover, tensile stresses are developed in carbon fiber. Hence, the fiber is broken in the matrix. With the result, the composite material showed catastrophic fracture behavior as it is difficult to pull out the fiber from the matrix. Further the composite materials exhibited a non-linear fracture behavior at $1600^0$C, because of creep in silicon carbide matrix. It is understood that the micro cracks contribute to the non-linear fracture mode of the composites by deflecting the crack growth. The interfacial bond in between the constituents of the composites depends on the properties of

interfacial phase and temperatures. The average value of shear strength obtained (Table 8) is 30 MPa. In the composites studied, no layer de-bonding is noticed. The average flexural strength obtained is observed to be 220 MPa. It gives an average work of fracture 26.58 kJ/m$^2$ for the 3D C-SiC specimens with 40% fiber volume fraction. It is observed that this value is four times that of two dimensional laminated ceramic materials. Also it is higher than that of laminated SiC composite (4.625 kJ/m$^2$) and much larger than monolithic ceramic material (Silicon Nitride, 80 J/m$^2$).

## 7. Conclusions

In the present work 3D C–SiC composites are prepared by LSI process using stitched preforms. The process for the fabrication of specimens is established with coal tar pitch impregnation into 3D carbon fiber preforms. The important conclusions drawn from the present work are:

1. The SEM micrographs reveal the uniformity of siliconisation and relatively less amount of un reacted silicon and carbon in the final composites.
2. It is also observed that the concentration of silicon in the composites is more at grain boundaries and at fiber bundles. This is because of slow diffusion of silicon into C-SiC in grains and relatively low availability of carbon in the fiber bundles compared to matrix bulk.
3. The mechanical properties of 3D C–SiC composites are determined experimentally. When fiber volume fraction is increased, fracture toughness and impact strength are increased correspondingly, which is proved by the experimental results obtained by conducting impact test as shown in Table 3.
4. The impact curve gives a lot of information about material properties. It also gives the information about the kind of fracture (brittle or nearly ductile) which is depicted graphically. The instrumented impact provides a better characterization of the material.
5. The experimental value of impact strength obtained for the sample Specimen No.4 with 40 % fiber volume fraction is 26.82 kJ/m$^2$ .
6. The maximum flexural strength obtained for the sample Specimen No.5 by conducting flexural test is 230.3 MPa.
7. The maximum shear stress from the experiment is observed to be 30.5 MPa.
8. The tensile strength obtained for the sample Specimen No.1 from the experiment is observed to be 70.2 MPa.

## References


[1] R. Naslain, Ceramic Matrix Composites, Chapman & Hall, London, 1992, 199-243.

[2] T.M. Besmann, B.W. Sheldon, R.A. Lowden, Vapor-Phase Fabrication and Properties of Continuous-Filament Ceramic Composites, Science, 253, 1991, 1104-1109.

[3] T. Ishikawa, S. Kajii, K. Matsanaga, T. Hogani, Y. Kohtoku, T. Nagasawa, A Tough, Thermally Conductive Silicon Carbide Composite with High Strength up to 1600°C in Air, Science, 282,1998, 1295–1297.

[4] K.M. Prewo, Fiber-Reinforced Ceramics: New Opportunities for Composite Materials, American Ceramic Society Bulletin, 68, 1989, 395-400.

[5] M. Wang, C. Laird, Damage and fracture of a crosswoven C/SiC composite subject to compression loading, Journal of Material Science, 31, 1996, 2065-2069.

[6] J.J. Brenann, Interfacial studies of chemical-vapor-infiltrated ceramic matrix composites, Material Science & Engineering A, 126, 1990, 203-223

[7] D. Singh, J.P. Singh, M.J. Wheeler, Mechanical Behavior of SiC(f)/SiC Composites and Correlation to in situ Fiber Strength at Room and Elevated Temperatures, Journal of the American Ceramic Society, 79, 1996, 591-596.

[8] S. Prouhet, G. Camus, C. Labrugee, A. Guette, Mechanical Characterization of Si–C(O) Fiber/SiC (CVI) Matrix Composites witrTa BN–Interphase, Journal of the American Ceramic Society, 77, 1994, 649-656.

[9] F.K KO, Preform Fibre Architecture for Ceramic-Matrix Composites, American Ceramic Society Bulletin, 68, 1989, 401-414.

[10] P. Pluvinage, A.P. Majidi, T.W. Chou, Damage characterization of two-dimensional woven and three-dimensional braided SiC-SiC composites, Journal of Material Science, 31, 1996, 232–241.

[11] Y.D. Xu, L.T. Zhang, Three-Dimensional Carbon/Silicon Carbide Composites Prepared by Chemical Vapour Infiltration, Journal of the American Ceramic Society, 80, 1997, 1897-1900.

[12] Y.D. Xu, L.T. Zhang, L.F. Cheng, D.T. Yan, Microstructure and mechanical properties of three-dimensional carbon/silicon carbide composites fabricated by chemical vapor infiltration, Carbon, 36, 1998, 1051-1056.

[13] Yongdong Xu, Laifei Cheng, Litong Zhang, Hongfeng Yin, Xiaowei Yin, Mechanical Properties of 3D fiber reinforced C/SiC composites, Material science & Engineering A, 300, 2001, 196-202.

[14] Per F. Perterson, Charles W. Forsberg, Paul S. Pickard, Advanced CSiC composites for high-temperature nuclear heat transport with helium, molten salt, and sulfur-iodine thermo mechanical hydrogen process fluids, Second Information Exchange meeting on Nuclear production of Hydrogen, Argonne National Laboratory, Illinois, USA, 2-3 October, 2003.